Myocardial Blood Flow, Metabolism, and Inotropic Reserve in Dogs with Dysfunctional Noninfarcted Collateral-Dependent Myocardium

Bernhard L. Gerber, MD[1]; Sarra Laycock, PhD[2]; Jacques A. Melin, MD[1]; Marcel Borgers, PhD[2]; Willem Flameng, MD[2]; and Jean-Louis J. Vanoverschelde, MD[1]

[1]*Division of Cardiology and PET Laboratory, University of Louvain Medical School, Brussels, Belgium; and*
[2]*Center for Experimental Surgery and Anaesthesiology, Catholic University of Leuven, Leuven, Belgium*

There is intense controversy as to the mechanisms underlying chronic but reversible left ventricular (LV) ischemic dysfunction. The aim of this study was to investigate the physiology underlying this condition in a canine model of noninfarcted collateral-dependent myocardium. **Methods:** Six mongrel dogs were instrumented with ameroid constrictors on the left circumflex and right coronary arteries and a partial occluder on the left anterior descending coronary artery. The animals were followed up for 6 mo. Every 6 wk, measurements of regional wall thickening (M-mode echo), myocardial blood flow (^{13}N-ammonia PET), oxygen consumption (^{11}C-acetate PET), and glucose uptake (^{18}F-FDG PET) were obtained. After 6 mo, myocardial blood flow reserve (during adenosine infusion) and regional contractile reserve (during infusion of a low dose of dobutamine) were also investigated. **Results:** Following ameroid implantation, regional thickening decreased in the posterior wall (to 34% ± 13% of baseline; $P < 0.001$) but not in the septum. Resting myocardial blood flow (56 ± 10 vs. 58 ± 15 mL · [min · 100 g]$^{-1}$), myocardial oxygen consumption (21 ± 3 vs. 22 ± 3 J · [beat · 100 g]$^{-1}$), and insulin-stimulated glucose uptake (39 ± 8 vs. 42 ± 11 μmol · [min · 100 g]$^{-1}$) were similar among dysfunctional and normal segments. Myocardial blood flow reserve was blunted in dysfunctional versus normal segments (3.7 ± 0.5 vs. 5.2 ± 1.5; $P = 0.06$). With dobutamine, wall thickening (to 69% ± 8% and 77% ± 11%, respectively) and oxygen consumption (to 36 ± 5 and 39 ± 5 J · [beat · 100 g]$^{-1}$, respectively) improved to the same extent in both segments. As a consequence, mechanical efficiency decreased in septal but remained unchanged in posterior segments during infusion of dobutamine. Biopsy specimens from both walls were free from any morphological alterations. **Conclusion:** Our data indicate that ameroid occlusion in dogs induces sustained reduction in regional contraction, which occurs despite normal levels of transmural blood flow and recruitable inotropic reserve. Since myocardial perfusion reserve was blunted, such perfusion–contraction mismatch could reflect repetitive stunning.

Key Words: Myocardial hibernation; canine model; ^{13}N-ammonia; ^{11}C-acetate; ^{18}F-FDG; PET

J Nucl Med 2002; 43:556–565

Received Jul. 2, 2001; revision accepted Dec. 18, 2001.
For correspondence or reprints contact: Jean-Louis Vanoverschelde, MD, Division of Cardiology, Cliniques Universitaires St. Luc UCL, Av. Hippocrate 10 / 2859, B-1200 Brussels, Belgium.
E-mail: vanoverschelde@card.ucl.ac.be

It is now widely accepted that patients with chronic coronary artery disease can experience prolonged regional ischemic dysfunction that does not necessarily arise from irreversible tissue damage and which, to some extent, can be reversed by restoration of blood flow (*1*). Because of its relevance to clinical cardiology (*2,3*), this form of chronic but reversible left ventricular (LV) dysfunction has attracted considerable interest in the mechanisms that underlie the phenomenon and the identification of clinical factors that may lead to its development. Unfortunately, for many years our understanding of the physiological mechanisms has lagged behind clinical descriptions because of a lack of appropriate animal models mimicking the human condition.

Recently, several investigators have reported on the successful development of chronic coronary stenosis or progressive ameroid occlusion models that result in chronic but reversible ischemic dysfunction. The results of these studies suggest that prolonged but reversible dyssynergy can arise through several different mechanisms, including chronic stunning and chronic hibernation. In one such study, it was recently shown that prolonged contractile dysfunction could be obtained in dogs instrumented with 2 ameroid occluders and a severe fixed coronary stenosis (*4*). Initial data obtained with this model indicated that the regional dysfunction progressively developed over time, that it persisted for up to 8 wk after instrumentation, and that it occurred despite normal rest perfusion. The aim of this study was to further characterize the physiology underlying the chronic contractile dysfunction observed in this model, focusing on longitudinal changes in glucose and oxidative metabolism, resting myocardial blood flow and flow reserve, and recruitable inotropic and oxidative reserve. An additional aim was to examine whether the observed dysfunction could be extended over longer periods of time, i.e., 6 mo.

MATERIALS AND METHODS

Animal Model

Seven mongrel dogs of either sex (19–25 kg) had instruments implanted in preparation for the experiments, as previously described (*4*). Briefly, under general anesthesia and sterile condi-

tions, the chest was opened at the fifth intercostal space, the pericardium was incised, and the heart was exposed. The proximal portion of the left anterior descending coronary artery, the left circumflex coronary artery, and the right coronary artery were dissected free 1–2 cm from their origins. A ring occluder, consisting of a portion of silicon tubing, was implanted around the left anterior descending coronary artery, proximal to the emergence of the first diagonal branch but after emergence of the first septal branch. The internal diameter of the tubing was chosen to reduce the vessel lumen by >75%. Two ameroid constrictors (Dimed Medical Engineering, Antwerp, Belgium) were also implanted, one on the left circumflex artery and one on the right coronary artery, proximal to any significant branch. The pericardium was closed and the chest was evacuated. All animals were routinely placed on antibiotic therapy (ampicillin, 16 mg/kg) for 10 d. The animals used in this study were maintained in accordance with the guidelines of the Ethical Committee of the University.

Experimental Protocol

Animals were studied serially, 1 wk before surgery and again at 6, 12, 18, and 24 wk after surgery. All studies were performed under general anesthesia to ensure stable hemodynamic conditions. After premedication with 0.4 mg fentanyl intramuscularly, animals were anesthetized with pentobarbital (10 mg/kg intravenously), intubated, and ventilated with room air. Anesthesia was maintained by continuous infusion of midazolam (1 mg/kg/h), supplemented with intravenous boluses of 0.1 mg fentanyl every hour. Two 18-gauge catheters were introduced into 2 separate foreleg veins for tracer injection and drug infusion and continuously perfused with saline. A 20-gauge catheter was introduced percutaneously into the left femoral artery for arterial pressure recordings. The ECG and the arterial pressure were continuously monitored throughout the experiments. For this purpose, serial 60-s ECG and pressure samples were digitized every 15 min and stored onto an HP1000 microcomputer for off-line analysis.

Studies were performed on 2 consecutive days under fasting conditions. On day 1, baseline measurements of regional mechanical function, perfusion, glucose uptake, and oxidative metabolism were obtained. On day 2, measurements of regional mechanical function and glucose uptake were again obtained, this time during hyperinsulinemic, euglycemic glucose clamp, as previously described (*5*). Glucose was coadministered at a rate adapted to maintain glucose plasma levels between 60 and 80 mg/dL throughout the study. Samples for insulin and free fatty acids were obtained at baseline and at the end of the glucose clamp.

In addition to the above measurements, at 24 wk, myocardial flow reserve and regional contractile reserve were also investigated. For assessment of myocardial flow reserve, regional myocardial blood flow was measured with PET and colored microspheres at baseline and during intravenous infusion of adenosine (140 μg/kg/min). For assessment of regional myocardial contractile reserve, measurements of regional myocardial wall thickening, blood flow, and oxidative metabolism were obtained at rest and again during intravenous administration of a low dose of dobutamine (1–5 μg/kg/min, adjusted to double the rate–pressure product). Subsequent to the completion of the low-dose steady state, dobutamine infusion rates were increased in 3-min dose increments to 40 μg/kg/min. Measurements of regional myocardial wall thickening were taken at each stage of the high-dose dobutamine protocol.

M-Mode and 2-Dimensional Echocardiography

Regional myocardial mechanical function was assessed using 2-dimensional guided M-mode echocardiography. Images were obtained from the right parasternal window with a Toshiba Sonolayer SSH140 (Toshiba, Zoetemeer, The Netherlands) equipped with a 2.5-MHz wide-angle phased-array transducer. M-mode recordings were obtained at the level of the papillary muscles, with the ultrasonic beam oriented perpendicularly to the mid-portion of the septal and posterior walls (between the papillary muscles). LV internal diameter and septal and posterior wall thickness were measured at end-diastole (R wave of the EKG) and end-systole (time of aortic valve closure). Septal and posterior systolic wall thickening was calculated as the difference between systolic and diastolic wall thickness and expressed as a percentage of diastolic wall thickness. Meridional end-systolic wall stress and regional mechanical work (*6*) were calculated by use of the following equations:

$$\sigma_m = \frac{1.33 \cdot LVP \cdot LVD}{4 \cdot Wth \cdot (1 + Wth/LVD)}, \qquad \text{Eq. 1}$$

$$RW = -\int \sigma_m \cdot d \ln (1/Wth), \qquad \text{Eq. 2}$$

where LVD = LV dimension (cm); LVP = LV pressure (mm Hg); RW = regional work (mJ/cm^3); Wth = wall thickness (cm); and σ_m = meridional wall stress (g/cm^2).

PET

PET was performed using an ECAT EXACT HR (CTI, Knoxville, TN) multislice tomograph with animals resting on the left side. After baseline hemodynamic and echocardiographic recordings, the animals were carefully positioned within the tomograph. After acquisition of attenuation data, emission data were acquired for each of the different tracers. Myocardial blood flow was assessed with ^{13}N-ammonia, myocardial oxidative metabolism with ^{11}C-acetate, and myocardial glucose uptake with ^{18}F-FDG. Tracers were injected intravenously by means of an infusion pump (model 351; Sage, Bromma, Sweden). As mentioned earlier, 2 FDG studies were performed on 2 consecutive days. The first study was performed in the fasting state; the second study was performed during hyperinsulinemic euglycemic glucose clamp.

Images were reconstructed on a UNIX microcomputer and reoriented into serial 9-mm-thick short-axis slices. Six large irregular volumes of interest were assigned to each of 4 consecutive short-axis slices encompassing mid- and basal levels of the LV myocardium. These volumes of interest were carefully drawn to closely match the echocardiographic segments. An additional circular volume of interest was assigned to the center of the LV blood pool. Counts were corrected for partial volume and spillover effects using a specially developed Monte Carlo simulation, as well as for dead-time losses (*7*). The quantitation of tomographic data was performed as previously described in our laboratory (*5*). Briefly, regional myocardial blood flow was quantified by use of a 3-compartment model. Regional myocardial oxidative metabolism was estimated by biexponential fitting of myocardial ^{11}C time–activity curves. Myocardial ^{11}C clearance rates were also expressed as myocardial oxygen consumption (MVO_2, $J \cdot [beat \cdot 100\ g]^{-1}$), using the relationship between MVO_2 and k_1 that had been delineated in studies of dogs under a wide range of pathophysiological conditions (hyperemia, increased workload, acute ische-

mia, reperfusion) (*8*). Regional mechanical efficiency was calculated as RW/MVO_2. Patlak graphic analysis was used to estimate absolute regional myocardial FDG uptake (*9*).

Microsphere Blood Flow

At 24 wk, regional myocardial blood flow was measured both with PET and the colored microspheres technique. Microspheres data were analyzed in 6 radial sectors from 2 basal and 2 midventricular cross-sections, using the same segmentation as with PET and echocardiography. Each sector was separated into a subepicardial and a subendocardial portion. Blood and tissue samples were analyzed with an automated sampling unit for spectrophotometric determination of dye intensity. This consisted of an exclusively designed flowcell (Hellma GmbH; Mullheim, Baden, Germany), a high-precision autosampling system, and a spectrophotometer (Beckman Instruments Inc., Fullerton, CA). Computer software created by the investigators was used to run these components simultaneously.

Coronary Angiography

At the end of the last experiments, selective coronary arteriography was performed from the right carotid artery to verify the occlusion of the right and left circumflex coronary arteries and the presence of a stenosis on the left anterior descending coronary artery. In all surviving animals, complete closure of the 2 ameroid constrictors was observed. In each case, a significant stenosis (50%–75%) was found on the proximal left anterior descending coronary artery after the emergence of the first septal branch.

Morphological Analysis

At the end of all measurements, the chest was opened and the heart was retrogradely perfused with a 2% glutaraldehyde in phosphate buffer at pH 7.4, excised, and sliced into serial 1-cm-thick short-axis slices, parallel to the atrioventricular groove. Transmural samples of glutaraldehyde-fixed myocardium from the septum and the posterior wall were analyzed by both light and electron microscopy. Light microscopy was used to quantify cellular alterations and the amount of fibrosis and to select regions of interest to be subsequently assessed with electron microscopy (*10*). Semithick sections stained with toluidine-blue and Periodic Acid Schiff reaction were obtained from each specimen. Each section was examined using a special grid dividing the field into 121 identical squares to measure the percentage of the biopsy surface covered by fibrosis or by cardiomyocytes. This procedure was repeated several times on different zones of the sample. Subsequently, 100–200 cardiomyocytes sectioned through the nucleus were examined and their morphological characteristics were studied (*10*). For the electron microscopic examination, the specimens were postfixed in osmium tetroxide and routinely embedded in epoxy resin.

Statistical Analysis

Continuous variables were expressed as mean ± 1 SEM. Comparisons between pre- and postoperative data were made by 2-level ANOVA for repeated measurements. Individual comparisons were performed posthoc by the Scheffé test. All tests were 2-sided, and a probability value of <0.05 was considered indicative of a statistically significant difference.

RESULTS

Contractile Dysfunction after Surgical Instrumentation

Of the 7 animals prepared for the experiments, 1 died suddenly of massive myocardial infarction 2 d after surgery. All 6 remaining animals survived and were successfully followed up during 6 mo. Baseline values for systemic hemodynamics and segmental wall thickening in the septal and posterior walls from the preoperative and the 4 postoperative studies are shown in Table 1. No significant changes in heart rate, mean blood pressure, or rate–pressure product were noted over the study period.

The time course of changes in systolic wall thickening is shown in Figure 1. In all dogs, systolic posterior wall thickening was decreased at 6 wk after surgery. Although the reduction in systolic posterior wall thickening persisted throughout the study period, its severity varied substantially between animals as well as over time in the same animal. Peak reduction in systolic posterior wall thickening occurred between 18 and 24 wk after surgery in all but one dog (dog #3). In this animal, systolic posterior wall thick-

TABLE 1
Hemodynamics and Segmental Ventricular Function

	Preoperative	Postoperative			
	Baseline	6 wk	12 wk	18 wk	24 wk
HR	51 ± 5	63 ± 9	56 ± 3	65 ± 7	53 ± 6
SBP	129 ± 5	123 ± 10	121 ± 5	134 ± 6	125 ± 6
mBP	86 ± 3	83 ± 10	83 ± 3	93 ± 5	83 ± 5
LVEDD	40 ± 2	41 ± 2	39 ± 1	39 ± 1	40 ± 2
Wth					
IVS	0.73 ± 0.09	0.72 ± 0.03	0.71 ± 0.08	0.82 ± 0.13	0.79 ± 0.08
PW	0.79 ± 0.07	0.40 ± 0.06*‡	0.50 ± 0.13	0.38 ± 0.08†‡	0.32 ± 0.04†§

*$P < 0.05$ vs. IVS.
†$P < 0.01$ vs. IVS.
‡$P < 0.05$ vs. baseline.
§$P < 0.01$ vs. baseline.
HR = heart rate (bpm); SBP = systolic arterial pressure (mm Hg); mBP = mean arterial pressure (mm Hg); LVEDD = LV end-diastolic dimension (mm); Wth = wall thickening (%); IVS = interventricular septum; PW = posterior wall.

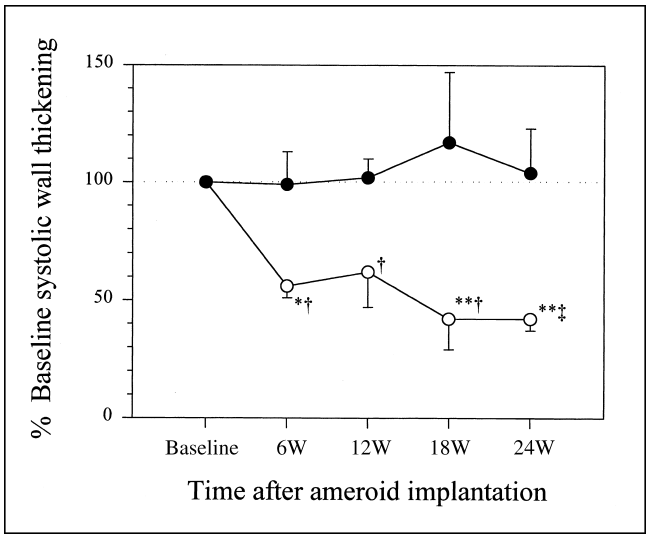

FIGURE 1. Time course of changes in systolic wall thickening in remote (●) and collateral-dependent (○) myocardium. Data are depicted as percent changes from baseline values obtained before ameroid implantation in the 5 dogs without infarction. *$P < 0.05$ vs. remote; **$P < 0.01$ vs. remote; †$P < 0.05$ vs. baseline; ‡$P < 0.01$ vs. baseline.

ening reached a nadir at 6 wk after surgery (24% of baseline) and recovered partially to 30% of baseline at 24 wk. Systolic wall thickening in the septal wall, which was not subtended by any coronary stenosis, remained unchanged throughout the study period.

Resting Myocardial Blood Flow and Its Relation to Regional Contractile Function

Resting myocardial blood flow was assessed by ^{13}N-ammonia PET every 6 wk during the 6-mo follow-up period. Mean values of transmural myocardial blood flow at 24 wk are shown in Table 2, whereas the time course of changes in transmural myocardial blood flow is shown in Figure 2. Before surgery, similar transmural myocardial blood flow values were measured in the septal and posterior walls. These values were again similar at 6, 12, 18, and 24 wk after surgery. After 24 wk of follow-up, colored microspheres were used to assess subendocardial and subepicardial blood flow. As shown in Figure 3, subendocardial blood flow was similar in the dysfunctional posterior wall and the normally contracting septal wall (64 ± 9 vs. 77 ± 7 mL · [min · 100 g]$^{-1}$; P = not significant). The endocardial-to-epicardial flow ratios (1.29 ± 0.16 vs. 1.03 ± 0.22; P = not significant) were also similar.

Data were analyzed also by comparing the posterior-to-septal-region ratio for blood flow with that for changes in wall thickening at baseline 6, 12, 18, and 24 wk after surgery (Fig. 4). At any time point, the decrease in segmental function was out of proportion to the possible decrease in transmural or endocardial blood flow, indicating perfusion–contraction mismatch.

Myocardial Flow Reserve

Myocardial flow reserve was measured with both PET and colored microspheres at the time of the terminal study. These measurements could not be obtained in 1 dog because of technical problems. Baseline transmural myocardial blood flow by PET was similar in the septal and posterior walls (64 ± 13 vs. 70 ± 13 mL · [min · 100 g]$^{-1}$; P = not significant). Hyperemic myocardial blood flow was significantly lower in the posterior than in the septal wall (227 ± 34 vs. 346 ± 35 mL · [min · 100 g]$^{-1}$; $P < 0.05$). Consequently, transmural myocardial flow reserve by PET was lower in the posterior than in the septal wall (3.7 ± 0.5 vs. 5.2 ± 1.5; $P = 0.06$). As shown in Figure 3, hyperemic endocardial and epicardial blood flow values measured with colored microspheres were significantly lower in the posterior than in the septal wall (128 ± 25 vs. 460 ± 84, and 363 ± 35 vs. 676 ± 125 mL · [min · 100 g]$^{-1}$, respectively; both $P < 0.05$).

Recruitable Inotropic and Oxidative Reserve

The evolution of regional myocardial oxidative metabolism in both walls is illustrated in Figure 5. Similar values of regional myocardial oxidative metabolism were measured in the septal and posterior walls before surgery and at 6, 12, 18, and 24 wk after surgery. Regional mechanical

TABLE 2
Systemic Hemodynamics, Mechanical Function, Myocardial Blood Flow, and Oxygen Consumption During Infusion of Dobutamine

	Baseline	Low-dose dobutamine
HR	54 ± 5	87 ± 8
mBP	83 ± 5	90 ± 4
Wth		
IVS	0.79 ± 0.08	0.77 ± 0.11
PW	0.32 ± 0.04†	0.69 ± 0.08§
RW		
IVS	5.6 ± 1.1	5.5 ± 1.1
PW	2.7 ± 0.2†	4.8 ± 0.7‡
MBF		
IVS	57 ± 10	155 ± 21§
PW	58 ± 12	145 ± 15§
MVO_2		
IVS	22 ± 3	39 ± 5§
PW	21 ± 3	36 ± 5*§
RW/MVO_2		
IVS	0.26 ± 0.03	0.14 ± 0.03§
PW	0.14 ± 0.02†	0.14 ± 0.02

*$P < 0.05$ vs. septum.
†$P < 0.01$ vs. septum.
‡$P < 0.05$ vs. baseline.
§$P < 0.01$ vs. baseline.
HR = heart rate (bpm); mBP = mean arterial pressure (mm Hg); Wth = wall thickening (%); IVS = interventricular septum; PW = posterior wall; RW = regional mechanical work (mJ/cm^3); MBF = transmural myocardial blood flow (mL · [min · 100 g]$^{-1}$); MVO_2 = myocardial oxygen consumption [J · [beat · 100 g]$^{-1}$).

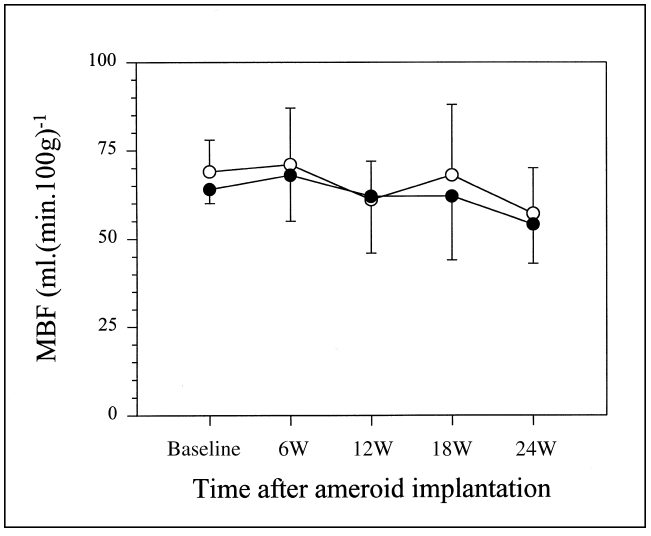

FIGURE 2. Time course of changes in transmural myocardial blood flow measured with PET in remote (●) and collateral-dependent (○) myocardium in the 5 dogs without infarction.

efficiency, defined by convention as the ratio of external mechanical work done to total energy supplied to and used by a given segment of the LV (RW/MVO_2), started to decrease in the posterior wall by 6 wk after surgery and reached a nadir at 24 wk (Fig. 6). Mechanical efficiency in the septal wall remained stable over time.

The changes in systemic hemodynamics, segmental wall thickening, myocardial blood flow, and MVO_2 resulting from the infusion of a low-dose (3.8 ± 0.5 μg/kg/min) of dobutamine are shown in Table 2. With low-dose dobutamine, systolic posterior wall thickening increased significantly, from 30% ± 4% to 69% ± 8%. By contrast, systolic septal wall thickening did not change significantly. Similar directional changes in regional mechanical work were noted. Myocardial blood flow and oxygen consumption increased to a similar extent in both walls. As a consequence of the respective changes in mechanical work and MVO_2, mechanical efficiency decreased in the septal wall but remained unchanged in the posterior wall during low-dose dobutamine infusion. Subsequent to the completion of the low-dose steady state, dobutamine infusion rates were increased up to 35 ± 5 μg/kg/min. This resulted in a further increase in heart rate (to 167 ± 10 bpm; $P < 0.001$) and rate pressure product (to 31,237 ± 3,301 bpm · mm Hg; $P < 0.001$). It also caused the reworsening of the posterior wall thickening (biphasic response).

Myocardial FDG Uptake Under Fasting and During Hyperinsulinemic Euglycemic Glucose Clamp

The evolution of regional myocardial glucose uptake under fasting conditions and during hyperinsulinemic euglycemic glucose clamp in both walls is illustrated in Figure 6. During the glucose clamp, blood insulin levels increased significantly (from 4 ± 1 μU/mL at baseline to 240 ± 25 μU/mL at end of procedure; $P < 0.001$), plasma glucose levels remained unchanged (from 70 ± 5 mg/dL to 70 ± 6 mg/dL; P = not significant), and the arterial concentration of fatty acid decreased (from 681 ± 208 μmol/L to 187 ± 73 μmol/L; $P < 0.001$). No significant differences in either fasted or insulin-stimulated FDG uptake were noted between the septal and posterior walls at any time point. On average, FDG uptake in the septum increased from 6 ± 4 μmol ·(min · 100 g)$^{-1}$ under fasting conditions to 42 ± 11 μmol ·(min ·100 g)$^{-1}$ during hyperinsulinemic euglycemic glucose clamp; whereas in the posterior wall, it increased from 6 ± 4 μmol · (min · 100 g)$^{-1}$ (P = not significant vs. septum) under fasting conditions to 39 ± 8 μmol · (min · 100 g)$^{-1}$ (P = not significant vs. septum) during hyperinsulinemic euglycemic glucose clamp.

Pathological Findings

In all 6 animals, pathology was examined at the time of the terminal study. Macroscopic and microscopic examinations revealed no evidence of necrotic lesions except in 1

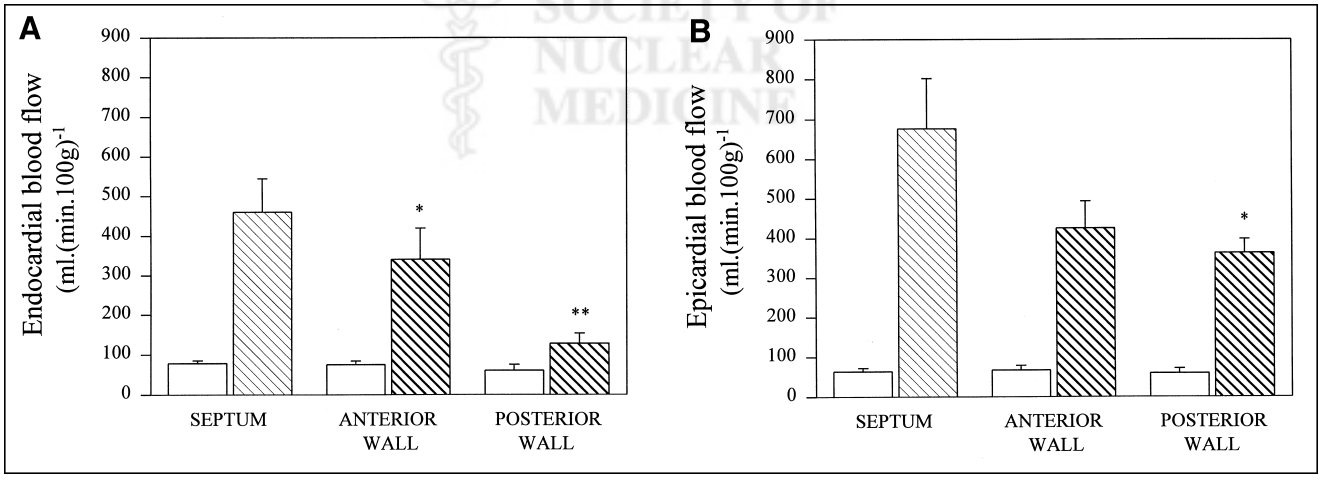

FIGURE 3. Endocardial (A) and epicardial (B) blood flows measured with colored microspheres in septum, anterior wall, and posterior wall, at baseline (open bars) and during maximal hyperemia (hatched bars) in the 5 dogs without infarction. *$P < 0.05$ versus septum; **$P < 0.01$ versus septum.

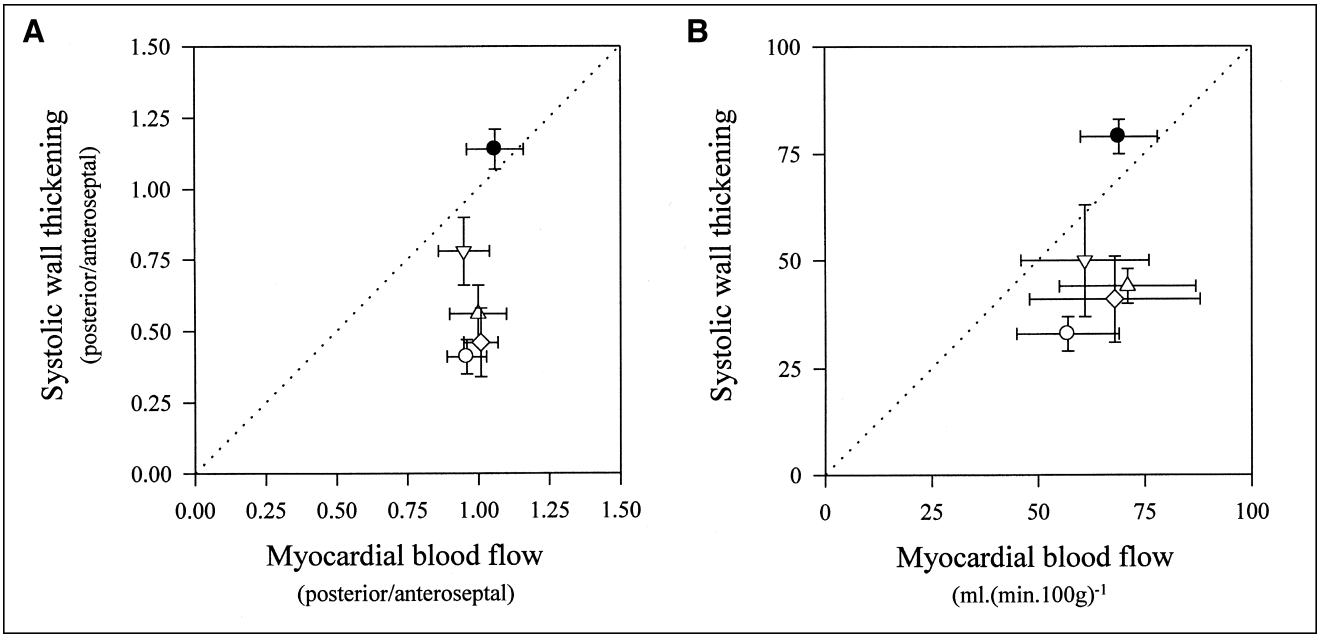

FIGURE 4. (A) Relation between blood flow (expressed as ratio of measurement in collateral-dependent region [posterior] compared with that in remote region [septal]) and systolic wall thickening in collateral-dependent region (expressed as a similar ratio). (B) Relation between absolute levels of myocardial blood flow and systolic wall thickening in posterior wall. Data are depicted before ameroid implantation (●) and 6 (△), 12 (▽), 18 (◇), and 24 (○) wk after ameroid implantation in the 5 dogs without infarction.

dog (dog #3), which showed a small subendocardial scar involving the inner fifth of the posterior wall. In the 5 remaining dogs, the surface of the biopsy occupied by extracellular matrix was not increased (1.19% ± 0.18%), and no structural changes affecting the cardiomyocytes were noted.

DISCUSSION

The aims of this study were to investigate the long-term outcome of dysfunctional noninfarcted collateral-dependent myocardium and to explore the underlying physiology, including glucose and oxidative metabolism, resting myocardial blood flow and flow reserve, and recruitable inotropic and oxidative reserve. The results can be summarized as follows:

1. Noninfarcted collateral-dependent myocardium exhibited mechanical dysfunction that developed around the presumed time of ameroid occlusion at 6 wk and remained relatively stable for up to 6 mo after ameroid implantation.

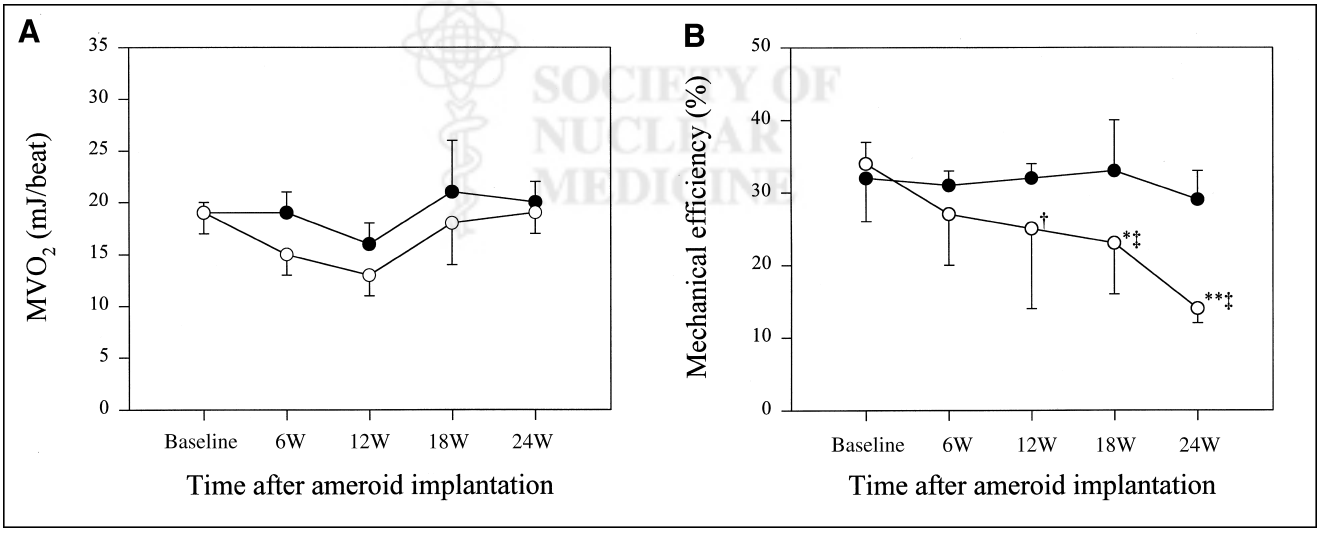

FIGURE 5. (A) Time course of changes in myocardial oxygen consumption measured with PET in remote (●) and collateral-dependent (○) myocardium. (B) Time course of changes in regional mechanical efficiency in remote (●) and collateral-dependent (○) myocardium. Data are from the 5 dogs without infarction. *$P < 0.05$ vs. remote; **$P < 0.01$ vs. remote; †$P < 0.05$ vs. baseline; ‡$P < 0.01$ vs. baseline.

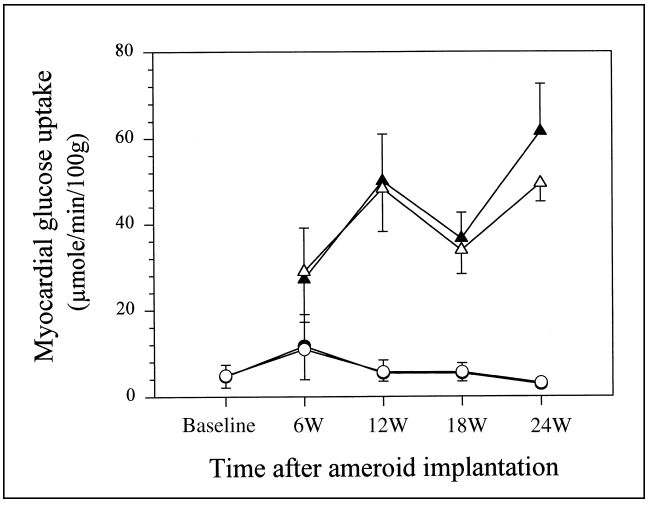

FIGURE 6. Time course of changes in myocardial glucose uptake measured with PET under fasting conditions (○,●) and during hyperinsulinemic euglycemic glucose clamp (△,▲) in remote (●,▲) and collateral-dependent (○,△) myocardium in the 5 dogs without infarction.

2. Dysfunctional collateral-dependent myocardium showed similar levels of resting myocardial blood flow and oxidative metabolism as remote normally contracting myocardium from the same animal.
3. Dysfunctional collateral-dependent myocardium showed reduced myocardial flow reserve compared with remote normally contracting segments.
4. FDG uptake under fasting conditions was similar and increased to a similar extent with insulin in dysfunctional myocardium as in remote normally contracting segments.
5. Dysfunctional myocardium displayed recruitable inotropic reserve when challenged by a low dose of dobutamine. Increases in myocardial blood flow and oxygen consumption paralleled the enhancement of myocardial function, which therefore does not result from improved mechanical efficiency. High doses of dobutamine resulted in the reappearance of contractile dysfunction (biphasic response).

The current study describes the chronic follow-up of an intact canine heart model with long-term coronary occlusion and sustained segmental dysfunction. A short-term follow-up (8 wk) of this same model was reported elsewhere (*4*). That study found that the systolic wall thickening of collateral-dependent myocardium started to decrease as early as 7 d after ameroid implantation, the presumed time when the ameroid constrictors would start to exert their stenotic effect. It was also found that regional function subsequently deteriorated further, albeit with large daily and individual variations. Contractile dysfunction then stabilized around the presumed time of complete coronary occlusion, about 5 wk after surgery.

Data from the current study extend these previous findings. Significant contractile dysfunction was noted as early as 6 wk after instrumentation, i.e., at the time of our first functional assessment. Contractile dysfunction subsequently persisted throughout the study, reaching its nadir at around 24 wk. At that time, systolic wall thickening in the ischemic area averaged 36% of baseline. Gross macroscopic examination of postmortem specimens showed no evidence of myocardial infarction, except in 1 animal, which exhibited a small subendocardial scar. As shown earlier (*4*), contractile dysfunction in this model is reversible, as it can be reversed by angioplasty of the ring stenosis of the left anterior descending artery.

Ameroids have been used in many instances to slowly occlude coronary arteries and produce collateral-dependent myocardium. In most prior studies, however, little or no reduction of contractile function in the collateral-dependent regions was observed (*11,12*), most likely because of the rapid collateralization that typically occurs in dogs after single ameroid implantation. To circumvent this problem, we implanted more than one ameroid constrictor and attempted to attenuate collateral blood flow by partially occluding the single remaining vessel able to provide collaterals, i.e., the left anterior descending coronary artery. Our model is thus quite similar to that recently described by Firoozan et al. (*13*), although in our study, the severity of dysfunction was somewhat less and did not result in overt cardiac failure. This is probably because the left anterior descending coronary artery remained patent in our study, whereas it was totally occluded in the study by Firoozan et al. Our results are also in agreement with those of other studies that used ameroid constrictors (*13–15*) and in which segmental dysfunction progressively developed around the fourth week after ameroid implantation. However, at variance with these previous studies, contractile dysfunction persisted for up to 6 mo in our study, whereas it was only transient in these earlier reports. Similarly prolonged reductions of contractile function were nonetheless reported recently after implantation of a ring stenosis in juvenile pigs (*16*).

There is intense controversy as to the mechanisms underlying chronic reversible ischemic dysfunction. One controversy currently relates to whether chronic contractile dysfunction simply reflects repetitive or chronic stunning, or whether the heart has the intrinsic capability to spontaneously downgrade its contractile function and energy requirements to cope with a sustained chronic reduction in myocardial blood flow, a condition that has been referred to as "myocardial hibernation." To elucidate potential pathophysiological factors associated with chronic dysfunction, one thus needs to examine regional flow–function relations in the area of dysfunction (*17*). To measure myocardial blood flow in this study, we used both PET, which allows measurement of transmural myocardial blood flow, and the colored microspheres technique, which permits computation of subendocardial blood flow. By using these 2 techniques at all times and especially when dysfunction was maximal, we found no differences in either transmural or

subendocardial blood flow between the dysfunctional and remote normally contracting segments, except in the 1 dog with a small subendocardial infarction. In all other animals, similar to the findings reported from an early time-course study (*4*), transmural and subendocardial blood flows were homogeneously distributed across the entire LV and remained so throughout the study period. A similar uncoupling between resting flow and function had been previously observed during the course of ameroid occlusion in dogs (*14*) and pigs (*15*) with prolonged albeit transient regional contractile dysfunction, and more recently in pigs with severe coronary artery stenosis (*18,19*). Our data are also consistent with previous observations in humans with dysfunctional noninfarcted collateral-dependent myocardium that showed nearly normal levels of resting transmural myocardial blood flow to the collateral-dependent area despite markedly reduced contraction (*10*).

Although the above findings allowed us to eliminate chronic perfusion–contraction matching as the cause of chronic regional dysfunction in our study, they do not provide definite clues as to the underlying mechanism. Since hyperemic vasodilatory reserve measured at the time of the terminal study was found to be significantly reduced in the dysfunctional area compared with remote normally contracting myocardium, it is tempting to hypothesize that the chronic dysfunction seen in noninfarcted collateral-dependent myocardium might have been the consequence of repetitive cumulative episodes of ischemia and reperfusion, resulting in a state of chronic stunning. Unfortunately, due to the design of our study, episodes of myocardial stunning could not be demonstrated. Nevertheless, arguments in favor of the implication of stunning include (a) the marked day-to-day variations observed during the early time course of this model (*4*); (b) the preservation of myocardial blood flow and oxygen consumption at rest; (c) the reduction in flow reserve; (d) the presence of a residual recruitable inotropic reserve; (e) the induction of high-demand ischemia during high-dose dobutamine infusion; and (f) the absence of morphological changes at pathology. Our hypothesis is also supported by results of studies that examined the time course of contractile dysfunction in chronic coronary stenosis (*4,13,20*) and progressive ameroid occlusion models (*15*). These studies have indeed shown that during the first weeks after onset of dysfunction, endocardial blood flow often remains normal or is only marginally decreased, and that severity of dysfunction correlates directly with reduction in subendocardial flow reserve but is unrelated to resting subendocardial blood flow (*20*). The fact that in some of the studies the onset of dysfunction was preceded by repeated episodes of acute demand-induced ischemia (*15*) further reinforces our hypothesis.

On the basis of the above studies, one could inadvertently conclude that the hibernating myocardium should always be equated to chronically stunned myocardium. Recent works by Fallovolita et al. (*21*) and Firoozan et al. (*13*) clearly challenge this point of view. Studying the time course of segmental blood flow in chronically dysfunctional myocardium, these authors indeed observed that, with time and increases in the physiological significance of the underlying coronary stenoses, some of the dysfunctional segments, which appeared "stunned" on early examination, eventually became underperfused. It is noteworthy that the transition from chronic stunning to chronic hibernation in these segments only occurred for threshold reductions in myocardial flow reserve. This dependence of the temporal progression to hibernation on critical reductions in myocardial flow reserve probably explains why, in some studies, chronic hibernation could never be induced, either because myocardial flow reserve progressively improved with time (*15*) or because it never became sufficiently reduced to produce hibernation, as in this study. Altogether, the experimental data suggest that chronic reversible myocardial ischemic dysfunction is a complex, progressive, and dynamic phenomenon that is initiated by repeated episodes of ischemia and in which resting perfusion, although initially preserved, may subsequently become reduced, probably in response to the decrease in myocyte energy demand. Indeed, the persistence of some degree of flow reserve, even when resting myocardial blood flow is reduced, suggests that the reduction in rest flow is somehow secondary to that in resting contractile function, and could serve as a way to increase residual myocardial perfusion reserve (*16*).

In addition to the above observations, previous experimental work has also shown that chronic but reversibly dysfunctional myocardium retained the ability to temporarily improve function on stimulation with catecholamines, whereas infarcted myocardium did not. The present study extends these earlier observations to the situation of chronic stunning. As expected from a previous work (*21*), infusion of dobutamine did not significantly affect the contractile performance of normal segments, but significantly decreased their mechanical efficiency. By contrast, low doses (3.8 ± 0.5 μg/kg/min) of dobutamine remarkably improved the contractile performance of chronically dysfunctional segments, which almost completely normalized. Interestingly, the improvement in mechanical function seen in dysfunctional segments with dobutamine was always attended by changes in both transmural myocardial blood flow and oxygen consumption of about the same magnitude, so that mechanical efficiency remained unchanged. The present findings thus suggest that the contractile reserve of the chronically dysfunctional myocardium depends mainly on maintenance of residual myocardial blood flow and oxidative reserve and not on changes in mechanical efficiency. This behavior thus appears to be somewhat different from what had been previously reported in acute stunning, in which inotropic reserve is at least partially dependent on changes in mechanical efficiency (*22,23*).

In this study, we also investigated possible changes in glucose metabolism in chronically dysfunctional myocardium. Previous studies in humans using PET and FDG had demonstrated that FDG uptake by such myocardium was

often greater under fasting conditions and responded somewhat less to insulin than that of remote normally contracting segments (*24,25*). This behavior is relatively similar to that of acutely stunned myocardium. In dogs undergoing 3 h of ischemia and reperfusion, Buxton et al. indeed found that although the relative FDG uptake of stunned segments was reduced compared with that of remote normal segments immediately on reperfusion, it progressively increased over time to remain higher than remote normal myocardium, 24 h after reperfusion (*26,27*). Similar results were obtained in patients with unstable angina (*28*) or recovering from exercise-induced ischemia (*29*). The results of this study are thus somewhat at variance with these earlier observations, as we found no differences in FDG uptake among dysfunctional and normally contracting segments, either under fasting conditions or during glucose clamp. Our results are nonetheless in agreement with those obtained in pigs instrumented with external constrictors (*30,31*). In these animals, the uptake of FDG indeed remained similar in reversibly dysfunctional and normally contracting segments for as long as myocardial flow reserve was not severely reduced. It is thus probable that the absence of metabolic derangements in our study was related to the lesser severity of the ischemic insult than in other studies (*20*).

The chronically dysfunctional canine myocardium described here shares both similarities and dissimilarities with human dysfunctional noninfarcted collateral-dependent myocardium, a condition previously considered to represent pure myocardial hibernation (*10*). Both are associated with normal or nearly normal levels of transmural myocardial blood flow at rest, and show normal or nearly normal levels of regional oxygen consumption (*10*); both have a preserved ability to increase regional myocardial FDG uptake in response to insulin stimulation (*10,24*); in both, regional myocardial perfusion reserve is significantly reduced (*10*); and both display recruitable inotropic reserve (*5*). Yet, the current model deviates from human hibernating myocardium in several respects. Specifically, the metabolic data under fasting conditions (*24,25*) and the tissue ultrastructure (*10*) are significantly different from what was shown to occur in humans. It is thus tempting to hypothesize that a spectrum of myocardial dysfunction actually exists in chronic but reversible ischemic dyssynergy; mild degrees of myocyte dysfunction being characterized by normal perfusion, little or no structural change, and normal FDG uptake, whereas more severe or more long-lasting forms of dysfunction would be associated with varying degrees of structural changes, resting underperfusion, and increase FDG uptake.

This study had several limitations. First, because we wanted to follow the animals over the long term and minimize the risk of infection, we intentionally limited the animal instrumentation to the implantation of 2 ameroid constrictors and 1 ring occluder. This obviously prevented us from continuously monitoring contractile function and firmly demonstrating the chronic stunning hypothesis. Second, to avoid undesirable movements during the long PET acquisitions, the animals were studied during general anesthesia. Although we carefully chose anesthetic drugs that do not interfere with myocardial function and metabolism, we cannot exclude the possibility that they somehow influenced the results. Finally, we measured perfusion and metabolism noninvasively with PET. Measurements by this technique are limited to transmural wall thickness, precluding the examination of endocardial and epicardial regions separately. The microspheres data nonetheless suggest that transmural heterogeneity only occurred during hyperemia, and not at rest.

CONCLUSION

We have studied a canine model of multiple coronary occlusions and stenosis, which resulted in chronic contractile dysfunction and was characterized by normal or nearly normal levels of resting myocardial blood flow and oxidative metabolism, reduced myocardial blood flow reserve, recruitable inotropic reserve, and maintained FDG uptake under both fasting conditions and hyperinsulinemic glucose clamp.

ACKNOWLEDGMENTS

We gratefully acknowledge the work of Raymond Bausart for technical assistance in tomographic acquisitions, and of our radiochemists, Benoît Georges and Daniel Labar, for radioisotope production. This study was supported by grants 3-4523-94 and 3-4540-95 from the Fonds National de la Recherche Scientifique et Médicale; by the Action de Recherche Concertée, grant 96/01-199; and by a grant from the Fonds de Développement Scientifique of the University of Louvain, Belgium.

REFERENCES

1. Rahimtoola SH. A perspective on the three large multicenter randomized clinical trials of coronary bypass surgery for chronic stable angina. *Circulation.* 1985;72 (suppl V):V123–V135.
2. Eitzman D, al-Aouar Z, Kanter HL, et al. Clinical outcome of patients with advanced coronary artery disease after viability studies with positron emission tomography. *J Am Coll Cardiol.* 1992;20:559–565.
3. Di Carli M, Sherman T, Khanna S, et al. Myocardial viability in asynergic regions subtended by occluded coronary arteries: relation to the status of collateral flow in patients with chronic coronary artery disease. *J Am Coll Cardiol.* 1994;23: 860–868.
4. Shivalkar B, Flameng W, Szilard M, et al. Repeated stunning precedes myocardial hibernation in progressive multiple coronary artery occlusion. *J Am Coll Cardiol.* 1999;34:2126–2136.
5. Gerber BL, Vanoverschelde JL, Bol A, et al. Myocardial blood flow, glucose uptake, and recruitment of inotropic reserve in chronic left ventricular ischemic dysfunction. Implications for the pathophysiology of chronic myocardial hibernation. *Circulation.* 1996;94:651–659.
6. Nakano K, Sugawara M, Kato T, et al. Regional work of the human left ventricle calculated by wall stress and the natural logarithm of reciprocal of wall thickness. *J Am Coll Cardiol.* 1988;12:1442–1448.
7. Vanoverschelde J-L, Melin J, Bol A, et al. Regional oxidative metabolism in patients after recovery from reperfused anterior myocardial infarction: relation to regional blood flow and glucose metabolism. *Circulation.* 1992;85:9–21.
8. Armbrecht JJ, Buxton DB, Schelbert HR. Validation of [1-(11)C]acetate as a tracer for noninvasive assessment of oxidative metabolism with positron emission tomography in normal, ischemic, postischemic, and hyperemic canine myocardium. *Circulation.* 1990;81:1594–1605.
9. Gambhir SS, Schwaiger M, Huang SC, et al. Simple noninvasive quantification

method for measuring myocardial glucose utilization in humans employing positron emission tomography and fluorine-18 deoxyglucose. *J Nucl Med.* 1989; 30:359–366.
10. Vanoverschelde JL, Wijns W, Depre C, et al. Mechanisms of chronic regional postischemic dysfunction in humans. New insights from the study of non-infarcted collateral-dependent myocardium. *Circulation.* 1993;87:1513–1523.
11. Tomoike H, Franklin D, Kemper WS, McKown D, Ross JJ. Functional evaluation of coronary collateral development in conscious dogs. *Am J Physiol Heart Circ Physiol.* 1981;241:H519–H524.
12. Tomoike H, Inou T, Watanabe K, et al. Functional significance of collateral during ameroid induced coronary stenosis in conscious dogs. *Circulation.* 1983; 67:1001–1008.
13. Firoozan S, Wei K, Linka A, et al. A canine model of chronic ischemic cardiomyopathy: characterization of regional flow-function relations. *Am J Physiol Heart Circ Physiol.* 1999;276:H446–H455.
14. Canty JM, Klock FJ. Reductions in regional myocardial function at rest in conscious dogs with chronically reduced regional coronary artery pressure. *Circ Res.* 1987;61(suppl II):107–116.
15. Shen YT, Vatner SF. Mechanism of impaired myocardial function during progressive coronary stenosis in conscious pigs. *Circ Res.* 1995;76:479–488.
16. Mills I, Fallon JT, Wrenn D, et al. Adaptive responses of coronary circulation and myocardium to chronic reduction in perfusion pressure and flow. *Am J Physiol Heart Circ Physiol.* 1994;266:H447–H457.
17. Ross J, Jr. Myocardial perfusion-contraction matching. Implications for coronary heart disease and hibernation. *Circulation.* 1991;83:1076–1083.
18. Bolukoglu H, Liedtke AJ, Nellis SH, et al. An animal model of chronic coronary stenosis resulting in hibernating myocardium. *Am J Physiol Heart Circ Physiol.* 1992;263:H20–H29.
19. Liedtke AJ, Renstrom B, Nellin SH, Hall JL, Stanley WC. Mechanical and metabolic functions in pig hearts after 4 days of chronic coronary stenosis. *J Am Coll Cardiol.* 1995;26:815–825.
20. Fallavolita JA, Canty JM. Differential ^{18}F-2-deoxyglucose uptake in viable dysfunctional myocardium with normal resting perfusion. Evidence for chronic stunning in pigs. *Circulation.* 1999;99:2798–2805.
21. Fallavollita JA, Perry BJ, Canty JM. ^{18}F-2-deoxyglucose deposition and regional flow in pigs with chronically dysfunctional myocardium. Evidence of transmural variations in chronic hibernating myocardium. *Circulation.* 1997;95:1900–1909.
22. Vanoverschelde JL, Wijns W, Essamri B, et al. Hemodynamic and mechanical determinants of myocardial oxygen consumption in the normal human heart: effect of dobutamine. *Am J Physiol Heart Circ Physiol.* 1993;265:H1884–H1892.
23. McFalls EO, Duncker DJ, Krams R, et al. Recruitment of myocardial work and metabolism in regionally stunned porcine myocardium. *Am J Physiol Heart Circ Physiol.* 1992;263:H1723–H1731.
24. Bergmann SR, Weinheimer CJ, Brown MA, Perez JE. Enhancement of regional myocardial efficiency and persistence of perfusion, oxidative, and functional reserve with paired pacing of stunned myocardium. *Circulation.* 1994;89:2290–2296.
25. Gerber BL, Melin JA, Bol A, Vanoverschelde JL. Attenuated response of myocardial glucose utilization to insulin stimulation in hibernating myocardium [abstract]. *Circulation.* 1995;92:313
26. Maki M, Luotolahti M, Nuutila P, et al. Glucose uptake in chronically dysfunctional but viable myocardium. *Circulation.* 1996;93:1658–1666.
27. Buxton DB, Schelbert HR. Measurement of regional glucose metabolic rates in reperfused myocardium. *Am J Physiol Heart Circ Physiol.* 1991;261:H2058–H2068.
28. Buxton DB, Mody FV, Krivokapich J, Phelps ME, Schelbert HR. Quantitative assessment of prolonged metabolic abnormalities in reperfused canine myocardium. *Circulation.* 1992;85:1842–1856.
29. Araujo LI, Camici P, Spinks TJ, Jones T, Maseri A. Abnormalities in myocardial metabolism in patients with unstable angina as assessed by positron emission tomography. *Cardiovasc Drugs Ther.* 1988;2:41–46.
30. Camici P, Araujo LI, Spinks T, et al. Increased uptake of F-18 deoxyglucose in postischemic myocardium of patients with exercise-induced angina. *Circulation.* 1986;74:81–88.
31. McFalls EO, Baldwin D, Palmer B, et al. Regional glucose uptake within hypoperfused swine myocardium as measured by positron emission tomography. *Am J Physiol Heart Circ Physiol.* 1997;41:H343–H349.